The structure of the GPIb–filamin A complex

Fumihiko Nakamura, Regina Pudas, Outi Heikkinen, Perttu Permi, Ilkka Kilpeläinen, Adam D. Munday, John H. Hartwig, Thomas P. Stossel, and Jari Ylänne

Filamin A (FLNa), a dimeric actin cross-linking and scaffold protein with numerous intracellular binding partners, anchors the platelet adhesion glycoprotein (GP) Ib-IX-V receptor to actin cytoskeleton. We mapped the GPIbα binding site to a single domain of FLNa and resolved the structure of this domain and its interaction complex with the corresponding GPIbα cytoplasmic domain. This is the first atomic structure of this class of membrane glycoprotein–cytoskeleton connection. GPIbα binds in a groove formed between the C and D β strands of FLNa domain 17. The interaction is strikingly similar to that between the β7 integrin tail and a different FLNa domain, potentially defining a conserved motif for FLNa binding. Nevertheless, the structures also reveal specificity of the interfaces, which explains different regulatory mechanisms. To verify the topology of GPIb-FLNa interaction we also purified the native complex from platelets and showed that GPIb interacts with the C-terminus of FLNa, which is in accordance with our biochemical and structural data. (Blood. 2006;107:1925-1932)

Introduction

Filamin A (FLNa), previously called actin-binding protein or ABP-280, is the major nonmuscle isoform of a family of extended dimeric proteins. FLNa subunits have a conserved actin-binding domain at their N-termini linked to 24 tandem filamin type immunoglobulin-like domains interrupted by 2 flexible hinges and dimerizing through the self-association of the ultimate C-terminal domain. Because of this unique structure, FLNa molecules can induce actin filaments into a 3-dimensional gel that represents a characteristic cortical actin structure.[1] Additional functions of FLNa are to anchor cell-surface receptors to the actin cytoskeleton and to scaffold cytoplasmic signaling proteins. Altogether, more than 50 interaction partners of FLN are known.[2,3] Human melanoma cells that do not express FLNa have impaired locomotion and unstable membranes that spasmodically bleb. Expression of FLNa restores the translational locomotion and reduces membrane blebbing.[4] Using these cell lines, impairments in functions ascribed to FLNa's binding to its many partners have been documented.[2] Furthermore, the importance of FLNa during development has become apparent from genetic analysis of a wide range of human diseases, the versatility of which highlights distinct FLNa-partner interactions.[5,6]

The glycoprotein (GP) Ibα is a component of the platelet von Willebrand factor (VWF) receptor identified as the first FLNa-binding partner 2 decades ago. The GPIb-V-IX receptor consists of 4 transmembrane subunits: GPIbα, disulfide-linked to GPIbβ, and the noncovalently associated GPIX and GPV components, in ratios of 2:2:2:1.[7] The cytoplasmic tails of GPIbα are attached to actin filaments by FLNa.[2,8,9] Previous work showed that the GPIbα cytoplasmic domain interacted with C-terminal domains of FLNa (domains 17-19)[10] and delimited the GPIbα binding site for FLNa to a short span of residues 557 to 575.[11]

The GPIbα-FLNa interaction is essential for the platelet adhesion to VWF that binds extracellular domain of the GPIb-V-IX receptor, for maintaining normal platelet integrity and shape, and for normal signal transduction reactions involved in platelet activation.[12,13] The absence of, or mutations in, VWF or in the GPIb-V-IX receptor are responsible for von Willebrand disease[14] or Bernard-Soulier syndrome,[15] respectively, disorders characterized by either bleeding or increased thrombosis. Additional roles of the GPIb-V-IX receptor in vascular biology have been recognized due to the identification of novel adhesive ligands for the receptor such as P-selectin, αMβ2 integrin, the coagulation factors thrombin and factors XI and XII, and the major extracellular matrix protein, collagen.[16] Rearrangements of the GPIb-IX-V receptor of platelets mediate the clearance by αMβ2 on Kupffer cells in the liver of platelets exposed to cold temperatures, a phenomenon that greatly affects clinical platelet transfusion technology.[17]

Because of its physiologic importance, we characterized the GPIbα-FLNa interaction in detail. Here we report mapping of the GPIbα binding site to the FLNa domain 17 (IgFLNa17), nuclear magnetic resonance (NMR) structure of this domain, and a crystal structure of the GPIbα peptide–IgFLNa17 complex. Collectively,

From the Hematology Division, Department of Medicine, Brigham and Women's Hospital, Harvard Medical School, Boston, MA; Biocenter Oulu and Department of Biochemistry, University of Oulu, Finland; Laboratory of Organic Chemistry, Department of Chemistry, and Institute of Biotechnology, University of Helsinki, Finland; Department of Biochemistry and Molecular Biology, Monash University, Clayton, Victoria, Australia; and Department of Biological and Environmental Science, University of Jyväskylä, Finland.

Submitted October 4, 2005; accepted October 23, 2005. Prepublished online as *Blood* First Edition Paper, November 17, 2005; DOI 10.1182/blood-2005-10-3964.

Supported by National Institutes of Health grants numbers 19429 (to T.P.S.) and 056252 (to J.H.H.) and the Academy of Finland grants numbers 51863, 202725, and 203675 (to J.Y.).

F.N. and R.P. contributed equally to this work.

The online version of this article contains a data supplement.

An Inside *Blood* analysis of this article appears at the front of this issue.

Reprints: Jari Ylänne, Department of Biological and Environmental Science, University of Jyväskylä, Survontie 9, FIN-40014 Jyväskylä, Finland; e-mail: jylanne@cc.jyu.fi; or Thomas P. Stossel, Hematology Division, Department of Medicine, Brigham and Women's Hospital, Harvard Medical School, 75 Francis St, Mid-Campus 3, Boston, MA 02115; e-mail: tstossel@rics.bwh.harvard.edu.

The publication costs of this article were defrayed in part by page charge payment. Therefore, and solely to indicate this fact, this article is hereby marked "advertisement" in accordance with 18 U.S.C. section 1734.

our data define the atomic structure of the GPIbα-FLNa interface. Recently, the crystal structure of the integrin β7–FLNa complex has also been solved[45] and the 2 structures reveal not only marked similarity, which potentially provides a motif for FLNa-partner complexes, but also specificity, which explains the regulatory mechanism for integrin β7 binding. Although previous reports suggested that the complex is tight, isothermal titration calorimetry analysis of IgFLNa17 and GPIbα556-577 peptide demonstrates that the tightness of the complex is explained only by engaging both sites on FLNa molecules with the corresponding alpha chains of a single VWF receptor. Finally, we report the electron micrographs of the native GPIb-FLNa complex from human platelets, the first visualization of a native complex of a transmembrane receptor with a cytoskeletal protein. The micrographs show that VWF receptor globules localize to a central position of the "V"-shaped filamentous FLNa dimer in accordance with the mapping data and suggest that complex is stable. Based on these data, we propose that the higher order (or topological) structure determines the tight-binding avidity of FLNa to the GPIb-IX-V receptor.

Materials and methods

Reagents

The antibodies, peptides, proteins, and DNA constructs used in this study are described in the supplemental experimental procedures (available on the *Blood* website; see the Supplemental Materials link at the top of the online article).

In vitro binding assay

Binding of recombinant proteins to the GPIbα was tested by mixing GST-GPIbα515-610 or GST with purified recombinant human FLNa fragments or whole protein in 400 μL binding buffer (20 mM Tris-HCl [pH 7.4], 150 mM NaCl, 0.1% [vol/vol] Tween 20, 1 mM EGTA) in the presence or absence of synthetic GPIbα556-577 peptide. After incubation at room temperature for 1 hour, 10 μL glutathione-Sepharose beads were added and further incubated for 30 minutes. The beads were washed 4 times with binding buffer and proteins were solubilized in sodium dodecyl sulfate (SDS) sample buffer. Proteins were then resolved by SDS–polyacrylamide gel electrophoresis (PAGE; 9.0% or 15.0% [wt/vol]) and stained with Coomassie brilliant blue. To test FLNa interaction with the synthetic GPIbα556-577 peptide (peptide precoupled to NHS-Sepharose 4B), the same process was repeated with the 5 μL beads per assay.

In vivo binding assay

Green fluorescent protein (GFP)–FLNa and its mutants were transiently expressed in CHO-GPIbαβ/IX cells.[18] After transfection (72 hours) the cells were rinsed with phosphate-buffered saline (PBS) and lysed in PBS containing 1% Triton X-100, 1 mM phenylmethylsulfonyl fluoride (PMSF), 5 mM EGTA, 1 mM EDTA, 1 μg mL^{-1} pepstatin A, 1 μg mL^{-1} aprotinin, and 1 μg mL^{-1} leupeptin. Cell lysates were centrifuged at 15 000*g* for 10 minutes. Lysates were precleaned with GammaBind Plus Sepharose (Amersham Biosciences, Piscataway, NJ) and incubated with 2 μg goat polyclonal anti-GPIbα antibody for 1 hour at 4°C followed by 30 minutes incubation with 20 μL GammaBind Plus Sepharose (50% slurry) at 4°C. Samples were washed 4 times with 500 μL ice-cold PBS containing 1% Triton X-100, 5 mM EGTA, and 1 mM EDTA, and resuspended in 30 μL 2 × sample buffer and heated for 7 minutes at 95°C. Proteins were resolved on 9% SDS-PAGE and transferred to PVDF membranes. Membranes were blocked with 5% nonfat milk in TTBS (20 mM Tris-HCl [pH 7.4], 140 mM NaCl, 0.05% Tween 20) for 1 hour and incubated with the primary monoclonal antibodies (mAbs) anti-GFP or anti-GPIbα for 2 hours. Immunoreactive bands were detected by enhanced chemiluminescence (Pierce, Rockford, IL).

NMR

NMR spectra were measured from ^{15}N- and $^{15}N/^{13}C$-labeled IgFLNa17 (residues 1863-1956) protein with Varian Unity INOVA 500 MHz (relaxation data at 23°C) and 800 MHz (all other spectra at 20 °C) spectrometers (Varian, Palo Alto, CA). All spectra were processed with VNMR (Varian) and analyzed with Sparky 3.106 (T. D. Goddard and D. G. Kneller, University of California, San Francisco). The structure calculations were made with the program CYANA 2.0[19,20] and further refined with AMBER 8.0 (D. A. Case et al, University of California, San Francisco, 2004). Details of the techniques are given in the supplemental experimental procedures.

Crystallization

A roughly equimolar mixture of IgFLNa17 and GPIbα556-577 peptide was crystallized in 1.75 M ammonium phosphate (pH 8.2), and the crystals were refined by microseeding. The dataset was collected at the European Synchrotron Radiation Facility (ESRF) beamline ID23-1 (Grenoble, France). The data were processed with the XDS program[21] (http://www.mpimf-heidelberg.mpg.de/~kabsch/xds/) and solved by molecular replacement with the Phaser program[22] (http://www-structmed.cimr.cam.ac.uk/phaser/). Arp/Warp 6.1.1[23] (http://www.embl-hamburg.de/ARP/) and O[24] (http://alpha2.bmc.uu.se/alwyn/) were used for the model building, and Refmac5[25] (http://www.ccp4.ac.uk/) for the refinement. Further details are given in the supplemental experimental procedures.

Coordinates

The coordinates for the final 20 NMR structures, the crystallographic coordinates, and structure factors have been deposited in the Protein Data Bank (accession nos. 2AAV and 2BP3),[43] and the resonance assignments in the BioMagResBank (accession no. 6730).[44]

Preparation of FLNa-GPIb complex from human platelets

Human platelets (2.5×10^{10} cells) were prepared from freshly drawn human blood as previously described[26] and lysed with 20 mL 20 mM Tris-HCl [pH 7.4], 100 mM NaCl, 1% Triton X-100, 10 mM EGTA, 100 μg mL^{-1} DNAseI, 2 mM PMSF, 10 μg mL^{-1} aprotinin, and 10 μg mL^{-1} leupeptin. After centrifugation at 20 000*g* for 30 minutes at 4°C, the supernatant fluid (20 mL) was loaded onto HitrapQ (5 mL; Amersham Biosciences) column. The column was washed with 50 mL 10 mM Tris-HCl [pH 7.4], 250 mM NaCl, 0.01% Triton X-100, and 0.5 mM EGTA, and the FLNa-GPIb complex was eluted with a 100 mL linear gradient of 100 to 600 mM NaCl in 10 mM Tris-HCl (pH 7.4), 0.01% Triton X-100, and 0.5 mM EGTA at a flow rate of 2 mL min^{-1}. Fractions containing the FLNa-GPIb complex (eluting around 480 mM NaCl) were pooled and absorbed on a mAb3-14–Sepharose (0.6 mL). After washing the column with 10 mL HNEC (10 mM HEPES-NaOH [pH 7.2], 200 mM NaCl, 0.1 mM EGTA, and 1.0% CHAPS) solution, the FLNa-GPIb complex was eluted with 4.5 mL GST-IgFLNa3 (5 mg mL^{-1} HNEC solution). The eluate was passed through glutathione-Sepharose (3 mL) to remove GST-IgFLNa3, and the FLNa-GPIb complex was absorbed on WGA-agarose (1 mL; Vector Laboratories, Burlingame, CA). After washing the column with 10 mL HNEC solution, the FLNa-GPIb complex was eluted with 6 mL 2.5% (wt/vol) *N*-acetylglucosamine in HNEC solution. The complex was concentrated to 0.2 mg mL^{-1} using an Amicon Ultra-15 (Millipore, Billerica, MA) with a molecular-weight cutoff of 50 000. For electron microscopy, 60 mM (final concentration) octyl α-D-glucopyranoside was added.

Electron microscopy

The structure of recombinant FLNa molecules and GPIb-FLNa complexes isolated from human platelets was determined in rotary shadowed specimens. Samples were applied to freshly cleaved mica, dried under vacuum, and shadowed with 1.0 nm of platinum at a 5° angle with rotation followed

by 4 nm of carbon at 90° without rotation (Cressington CFE-60 apparatus, Cressington, Watford, United Kingdom). Metal replicas were floated in distilled water, picked up on 200 mesh carbon grids, and examined and photographed in a JEOL JEM-1200 EX electron microscope at an accelerating voltage of 80 kV as previously described.[27] Electron micrographs were digitized on an Epson 1680 scanner at 1200 dpi and printed from Adobe Photoshop version 7.0 (Adobe Systems, San Jose, CA).

Results

The cytoplasmic domain of GPIbα interacts with FLNa domain 17 in vitro

To characterize the interaction of GPIbα and FLNa in more detail, we performed in vitro reconstitution and competition assays using recombinant protein and synthetic peptides. A GST fusion protein encompassing residues 515 to 610 of the cytoplasmic tail of GPIbα bound to FLNa. A synthetic 22-mer peptide (hereafter designated GPIbα556-577), including the previously defined FLNa-binding site[11,28] (Figure 1A), completely inhibited this binding (Figure 1B) and also efficiently bound full-length FLNa when immobilized on Sepharose beads (Figure 1C). Figure 1D shows that GST-fusion proteins representing IgFLNa17 and 19, but not 18, bound to GPIbα556-577 beads. Untagged IgFLNa constructs also bound GPIbα515-610, but IgFLNa17 bound with a higher apparent affinity than IgFLNa19 (Figure 1E). Isothermal titration calorimetry demonstrated that GPIbα556-577 has affinity to IgFLNa17 (K_d = 11 μM; Figure S1). Furthermore, IgFLNa19 did not bind GPIbα515-610 in the presence of a 1:1 molar mixture with IgFLNa17 (Figure 1F). Most important, IgFLNa17, but not IgFLNa19, competed with full-length FLNa for binding to GST-GPIbα515-610 (Figure 1G). Taken together, the results indicate that IgFLNa17 is the major binding site for GPIbα.

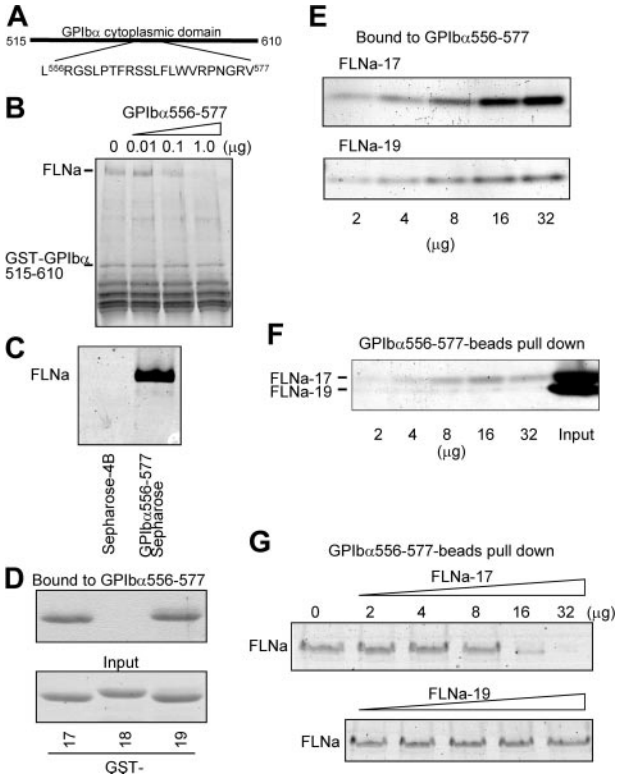

Figure 1. Identification of protein domains responsible for GPIbα/FLNa interactions. (A) Amino acid sequence of the synthetic 22-mer peptide (GPIbα556-577) that binds FLNa and was used for crystallography. (B) Binding of purified recombinant human FLNa (2 μg 400 μL^{-1}) to GST-GPIbα515-610 (5 μg 400 μL^{-1}) is inhibited by the 22-mer peptide, GPIbα556-577, in a dose-dependent manner. (C) Full-length FLNa (2 μg 400 μL^{-1}) binds the GPIbα556-577 peptide immobilized on Sepharose 4B but not Sepharose 4B alone. (D) In vitro binding of GST-IgFLNa17, -18, and -19 (2 μg each) to the GPIbα556-577 peptide beads. Top and bottom rows indicate bound and input proteins to GPIbα556-577, respectively. (E) Tag-free IgFLNa17 binds GPIbα556-577 peptide with higher affinity than IgFLNa19. Increasing amount of purified IgFLNa17 or -19 were incubated with GPIbα556-577 peptide beads. (F) IgFLNa17 is the major binding site for GPIbα556-577 peptide. Various amounts of IgFLNa17 and 19 at 1:1 molar ratio were incubated with GPIbα556-577 peptide beads in the pull-down experiment shown. (G) FLNa17 but not FLNa19 interferes the binding of full-length FLNa to GPIbα peptide beads. Various amounts of FLNa17 or -19 were mixed with 1 μg purified full-length FLNa and then incubated with GPIbα556-577 peptide beads. (B-G) Bound proteins were resolved by SDS-PAGE, and stained with Coomassie blue.

Table 1. NMR restraints

Total distance restraints	937
Per residue	9.6
Short-range, |i – j| less than or equal to 1	500
Medium-range, |i – j| between 1 and 5	68
Long-range, |i – j| greater than or equal to 5	369
Violation statistics	
Average AMBER energy, kcal mol^{-1}	−3115.0 ± 56.5
Average restraint violation energy, kcal mol^{-1}	20.54 ± 5.19
Maximum NOE restraint violation, Å	0.53
No. NOE violations greater than 0.3 Å	0.5 ± 0.5
Average RMS deviations from ideal covalent geometry	
Bonds, Å	0.0116 ± 0.0004
Angles, °	2.46 ± 0.09
Ramachandran diagram, %	
Most favored	74.4
Additionally allowed	22.6
Generously allowed	2.4
Disallowed	0.6
Ramachandran Z score	−0.510
Atomic coordinate RMSDs, Å	
Residues 1868-1954	
Backbone	0.92 ± 0.20
Heavy atom	1.33 ± 0.19
Residues 1868-1890, 1899-1911, 1919-1954	
Backbone	0.56 ± 0.08
Heavy atom	0.94 ± 0.07

Where applicable, values are ± SD.
i – j indicates the difference of residue numbers in protein sequence; RMSD, root mean square deviation.

The structure of FLNa domain 17 determined by NMR

The structure of free IgFLNa17 was solved by high-resolution solution state NMR spectroscopy (Table 1). A family of 20 structures is presented in Figure 2A. The structure consists of a β-sandwich of relatively straight 3- and 4-strand β-sheets (Figure 2A) resembling other FLN-type immunoglobulin-like domains (Table S1). In all, the solution structure of the domain is well defined (Table 1), but it contains 2 relatively loose loops close to the domain N-terminus (loops BC, DE; Figure 2A). In the case of loop BC this can be explained by a structural flexibility, which is visible in the absence of long-range nuclear Overhauser effects (NOEs), and is revealed by the relaxation time measurements (Figure S2B). The absence of long-range NOEs in the protruding loop DE leaves its structure ill-defined (Figure S2A). The titration of a ^{15}N-labeled IgFLNa17 sample with the GPIbα556-577 peptide

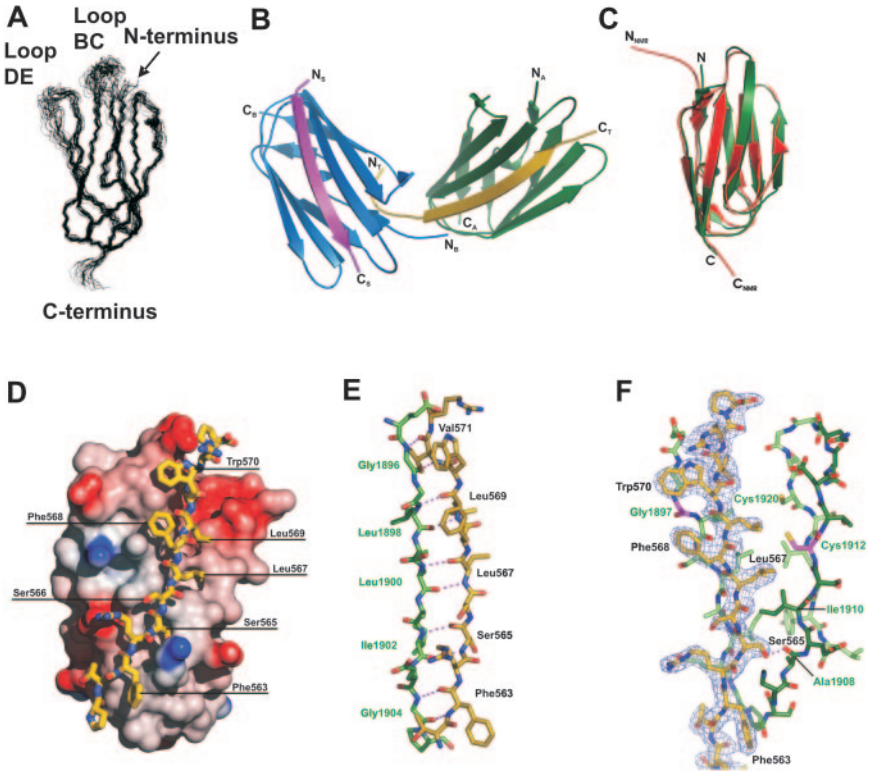

Figure 2. Structure of IgFLNa17 alone and in complex with the GPIbα peptide. (A) A family of 20 NMR structures of the IgFLNa17 in solution. (B) Asymmetric unit of the crystal. Two molecules of IgFLNa17 are colored green and blue (chains A and B, respectively). The GPIbα peptides are magenta (chain S) and gold (chain T). The N and C termini of all chains are shown. Note that the peptide T interacts with both FLN molecules. (C) Superimposition of the crystal structure (green) and the mean NMR structure (red). (D) Surface properties of the FLNa-GPIbα556-577 interaction. The accessible surface of IgFLNa17 has been colored according to surface potential and the peptide is shown on the top (gold and atom color). This representation shows the extended conformation of the peptide in the complex and the hydrophopic character of the interaction. (E) Main chain hydrogen bonding between the peptide (green) and IgFLNa17 strand C. (F) Details of the peptide interaction. An electron density map calculated with the final model without the peptide at the σ level of 1.4 shows that the side chains of the peptide are well defined. The G1897 and C1912 residues of FLNa that were mutated in subsequent studies are shown in magenta. Residue numbers for the peptide are shown in black and for FLNa in green.

showed that the peptide interaction with IgFLNa17 was in slow exchange in the NMR time scale. Thus, the binding could not be followed directly by observing chemical shift changes in the ^{1}H-^{15}N HSQC spectrum of the IgFLNa17 (data not shown), and would have required a full assignment for the spectra of the complex form. This was not pursued further, as parallel crystallization efforts for the complex form proved to be successful.

The crystal structure of FLNa domain 17 in complex with the GPIbα peptide

Well-diffracting crystals were obtained from cocrystallization experiments of IgFLNa17 with the GPIbα556-577 peptide. The structure of the complex was solved by molecular replacement with a model from the IgFLNc24,[29] and refined by using data to 2.3 Å resolution. The final model had good quality indicators and stereochemistry (Table 2). The asymmetric unit of the crystal contained 2 molecules of the IgFLNa17 and peptides binding to each of them (Figure 2B). The 2 molecules were refined independently and revealed structures and interactions very similar to the GPIbα peptide. The difference was that the peptide T (IgFLNa17 chains A and B as well as peptide chains T and S are indicated in Figure 2B) binding to molecule A also interacted through its N-terminus with the molecule B. In the peptide S, the N-terminus was disordered in the crystal and not visible in the electron density. Our interpretation is that the interaction between the peptide that is the same in both molecules represents the physiologic interaction between the native proteins, and that the binding of the peptide T to molecule B is specific for the crystal arrangement. Interestingly, the IgFLNa17 does not undergo any major structural rearrangements during GPIbα556-577 peptide binding, as the IgFLNa17 structures are essentially identical in both solution state (NMR) and in the complex form (x-ray) structures (Figure 2C).

In the crystal structure of the complex, residues 560 to 573 of the GPIbα peptide (LPTFRSSLFLWVRP) interact with the β strands C and D of IgFLNa17, and form a hydrogen-bonded β strand next to strand C of IgFLNa17 (Figure 2D-E). The segment of the peptide adopting this conformation is flanked by 2 proline residues (Pro561 and Pro573). In addition to main-chain hydrogen bonding (Figure 2E), a side-chain hydroxyl group of Ser565 makes a hydrogen bond with the main-chain O atom of Ala1908 (Figure 2F). On the FLNa side, the interface contains 43% polar and 57% nonpolar atoms. The main hydrophobic contacts are between Leu567 (13.27% of the contact surface area) of the peptide and Ile1910 and Cys1912 at strand D of FLNa. Also Phe563 (11.21%), Leu569 (9.67%), Val571 (13.67%), Phe568 (5.44%), and Trp570 (6.52%) of the peptide make remarkable hydrophobic contacts with FLNa (Figure 2D). These findings are consistent with previous observations that mutations of Phe568 and Trp570 abolish the binding of GPIbα to FLNa.[28] Furthermore, the association between GPIbα and FLNa resists chaotropic solvents over a wide pH range, although sodium dodecyl sulfate can separate the complex.[30] This behavior is consistent with the many hydrophobic contacts in the FLNa-GPIbα interface.

Point mutations in domain 17 of full-length FLNa disrupt the GPIb/FLNa interaction in vivo

To test if the GPIb complex interacts with FLNa through its IgFLNa17 in vivo, we engineered point mutations in IgFLNa17 residues (Gly1897, Ile1910, and Cys1912) that are located close to the peptide-FLNa interface seen in the crystal structure (Figures 2F and 3A). A fusion protein consisting of maltose-binding protein and IgFLNa17 or the I1910M mutant bound indistinguishably to GPIbα556-577 (Figure 3B). However, mutations G1897D or C1912D reduced binding, and the double mutant did not bind at all (Figure 3B). NMR spectroscopy confirmed that the double mutant caused no major defects in folding of the domain (data not shown). We also expressed GFP-tagged full-length human FLNa in the CHO-GPIbαβ/IX cells that stably express GPIbαβ/IX complex,[18] and were able to bring down FLNa with the GPIbαβ/IX complex (Figure 3C). Double-mutant (G1879D and C1912D) GFP-FLNa constructs

Table 2. Crystallographic data collection statistics

Wavelength, Å	0.9795
Beamline	ID23-1*
Crystal to detector distance, mm	275.91
Space group	P212121
Unit cell parameters, Å	
A	41.90
B	62.80
C	122.80
Resolution range, Å	19.88-2.32
R	8.7
I/Sigma (I)	14.08 (3.13)†
Completeness, %	86.9 (56.7)†
Redundancy	6.024 (3.7)†
Final model statistics (refinement)	
Resolution limits, Å	19.88-2.32 (2.375-2.315)†
No. reflections used for refinement	12 211
No. reflections in the test set	645
R, %	21.35
R_{free}, %	25.55
RMSD bonds/angles, Å/°	0.012/1.463
No. residues in Ramanchandran	244
Residues in most favored regions, %	87.7
Residues in additional allowed regions, %	12.3
Residues in generously allowed regions, %	0
No. protein atoms	1 537
No. water atoms	28
Average B factor, Å^2	58.354
B factor from Wilson plot, Å^2	52.0

I/Sigma (I) indicates reflection intensity divided by its measurement error; R, residual $R=(\Sigma||F(obs)|-k|F(calc)||)/\Sigma|F(obs)|$;$R_{free}$, R for the 5% of reflections not included in the refinement.

*ESRF, Grenoble, France.

†The values in parentheses are given for the highest resolution bin.

expressed at levels equivalent to endogenous FLNa in CHO cells did not associate at all with GPIbαβ/IX (Figure 3C), confirming that IgFLNa17 is also the major GPIbα-binding site in vivo.

N-ethylmaleimide (NEM) treatment (thiol alkylation of cysteine residues) dissociates FLNa from the GPIb complex in detergent-extracted platelets.[32] Figure 3D shows that NEM also dissociated endogenous FLN expressed in CHO-GPIbαβ/IX cells. NEM also inhibited IgFLNa17 binding to the GPIbα556-577 peptide (data not shown). This is consistent with the Cys[1912] and Cys[1920] residues locating at or near the binding interface as seen in the crystal structure (Figure 2F). Thus, NEM inhibition and the mutagenesis results confirm that the interface seen in the crystal is also functional in solution and in vivo and that IgFLNa17 is the major interaction site for GPIbα.

Electron microscopy of the GPIb-FLNa complex prepared from human platelets

To investigate its intact structure, the native GPIb-FLNa complex was purified from human platelets using affinity ligands, anti-FLNa mAbs and wheat germ agglutinin (WGA) immobilized on beads to ligate FLNa and GPIb, respectively. When the purified complex was examined by SDS-PAGE, Coomassie blue stained exclusively the FLNa subunits (Figure 4B, left blot). However, immunoblotting with anti-GPIbα mAbs demonstrated the presence of GPIbα in the purified complex (Figure 4B, center blot). Subsequent immunoblotting of the same membrane with anti-FLNa mAb showed a nearly equal ratio of GPIbα to FLNa (Figure 4B, right blot). In rotary shadowed images, the purified GPIb-FLNa complexes were monodisperse (Figure 4C). As previously described for purified FLNa molecules, semiflexible filamentous strands connect at one end to assume a "V"-shape (Figure 4C, top row). The FLNa-GPIb-IX-V complexes appeared similar, except for their decoration by globules of 22.6 ± 3.7 nm in diameter (mean ± SD; n = 50) localized to a central position of the FLNa molecules (Figure 4C, bottom row). Given that FLNa molecules dimerize at the carboxy-terminus of each chain, and that the purified GPIb-IX complex has globular domains of comparable size (~15.9 and ~8.9 nm),[33] the images are consistent with the localization of the GPIb-IX-V interaction site to C-terminus of FLNa (IgFLNa17-19),[10] and with the general schematic depiction of how the complex holds together (Figure 4A).[34]

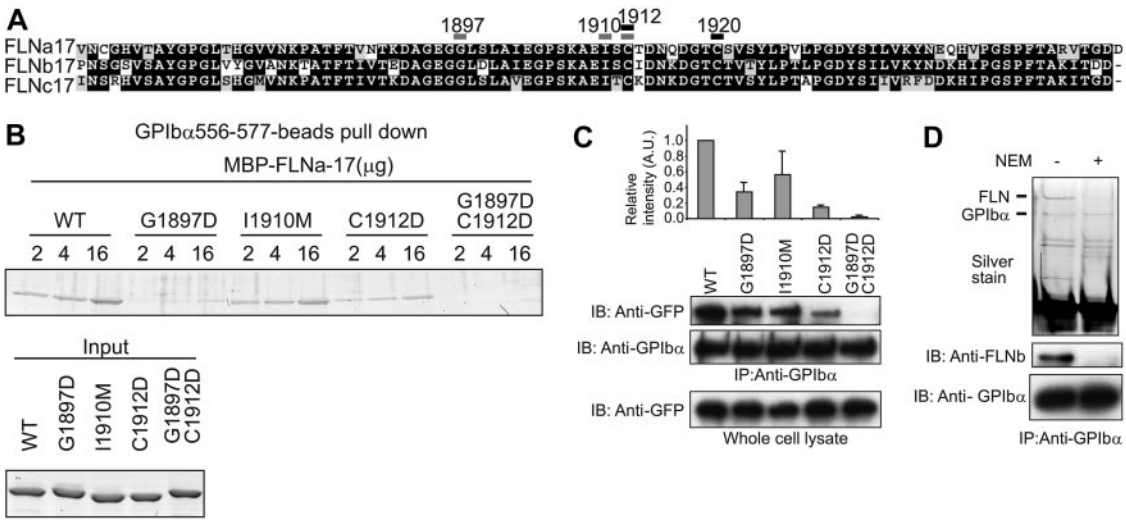

Figure 3. Obliteration of the binding of full-length FLNa to the GPIb complex in CHO cells by the point mutations in IgFLNa17 and by thiol alkylation. (A) ClustalW alignment[31] of domain 17 of FLN isoforms. Residues inferred from the atomic structure to be involved in interactions with GPIbα and tested by mutagenesis are indicated by the gray bars. Potential targets of NEM are indicated by the black bars. (B) Double mutations at G1897D and C1912D of IgFLNa17 abolish IgFLNa17/GPIb binding. Increasing amounts of purified MBP-IgFLNa17 (WT, wild type) and its mutants (G1897D, I1910M, C1912D, and G1897D+C1912D) were incubated with GPIbα556-577–peptide beads, and bound proteins were detected by SDS-PAGE followed by Coomassie blue staining. (C) GFP-FLNa and its mutants were expressed in CHO-GPIb/IX cells and coimmunoprecipitated with the GPIb-IX complex. GFP-FLNa is detected by immunoblot with anti-GFP mAb. The intensity of the band was analyzed by densitometry and the relative intensity graphed. Data are presented as mean ± SD of 3 independent experiments. (D) FLN is expressed in CHO-GPIb/IX cells and coimmunoprecipitated with the GPIb-IX complex. The linkage is uncoupled by treating the cell lysate with cystein-blocking reagent, NEM. Since only anti-FLNb, but neither anti-FLNa nor anti-FLNc antibodies available cross-react with hamster FLN, immunoblot was performed with anti-FLNb mAb (1-11c). IP indicates immunoprecipitation; IB, immunoblot.

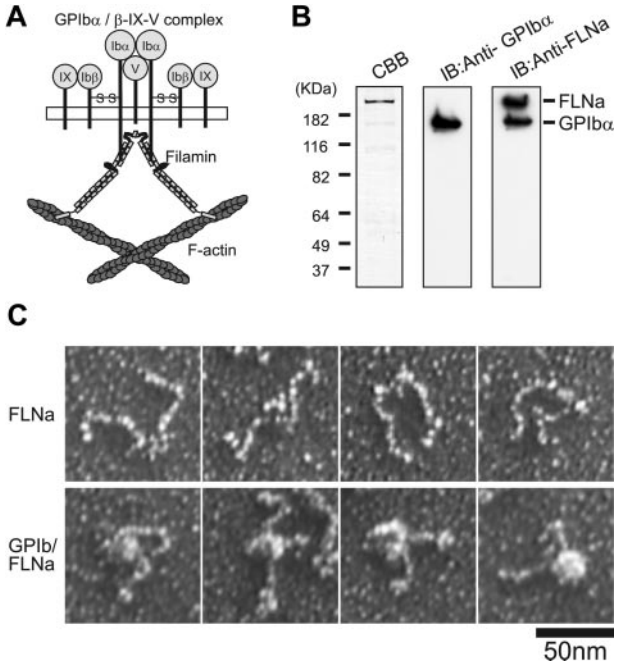

Figure 4. Schematic drawing and electron micrograph of the GPIb-FLNa complex from human platelets. (A) The cytoplasmic domain of GPIbα of the GPIb-IX-V complex binds to actin filaments through FLNa. (B) GPIb-FLNa complex from human platelets. Coomassie-blue-stained SDS-PAGE (10%) of a concentrated GPIb-FLNa complex (left). Immunoblot of the GPIb-FLN complex with anti-GPIbα mAb (WM23) (center). The same blotting membrane was subsequently blotted with an anti-FLNa mAb 3-14 (right). (C) Electron micrographs of rotary-shadowed recombinant FLNa molecules (top) and GPIb-FLNa complexes (bottom).

Discussion

The GPIb-IX-V receptor interacts with FLNa through IgFLNa17

The GPIbα binding site has been previously mapped to a FLNa fragment consisting of IgFLNa17-19.[10] Here we have further narrowed this region and showed that IgFLNa17 is the main interaction site, while IgFLNa19 has some affinity. Our competition experiments clearly showed that IgFLNa17 has a higher affinity for the GPIbα556-577 peptide than IgFLNa19 and that IgFLNa17 can compete with full-length FLNa for binding to the peptide, whereas IgFLNa19 cannot. Furthermore, specific point mutations of IgFLNa17, designed according to the crystal structure, prevent full-length FLNa binding to GPIb in coimmunoprecipitation experiments. Our electron microscope images of the GPIb-FLNa complex were fully consistent with the interaction site residing close to the C-terminus of the FLNa subunit.

The hydrophobic CD face of FLNa domains is a common binding interface for the GPIb and integrin

The crystal structure of the IgFLNa17-GPIbα556-577 peptide complex revealed that the peptide interacts with β-strands C and D of the IgFLNa17. The peptide forms a β-strand that is hydrogen-bonded to strand C and has several hydrophobic contacts with residues of both strands C and D. Apparently both the hydrophobic contacts and hydrogen bonding define the specificity of the interaction. It is interesting that the interaction of GPIbα with IgFLNa17 is very similar to that of integrin β7 cytoplasmic tail peptide with IgFLNa21.[45] Although the overall similarity is very low between the GPIbα and integrin cytoplasmic domains, the FLNa interaction sites are in both cases flanked by Pro residues, contain conserved Phe/Tyr and Ser residues, and take a β strand conformation in the complex (Figure 5). The β strand is associated with the strand C of the IgFLN in both cases, and conserved, but not identical, hydrophopic residues point toward strand D. Interestingly, IgFLNc24 also self-associates via β strands C and D, and we predicted that this is a common dimerization interface for all mammalian FLNs.[29] Our present results allow us to generalize even further and suggest that the CD face of the immunoglobulin sandwich is a common interaction surface for IgFLN domains and their partners. For example, the primary structure of this interface of IgFLNa17 is highly conserved in the corresponding domains of other FLN isoforms (FLNb and FLNc; Figure 4A), and FLNb is known to interact with GPIbα.[35,36] Despite the finding of many FLN-binding partners, one of the major issues of FLN research is that critical information of the biological significance of their individual interaction is limited because in most cases the binding sites have not been narrowed down to a single IgFLN domain or to a short sequence on the partner. Although it is still too early to define the "FLN-binding motif" of FLN-binding partners with 1 GPIbα and 4 β-integrin sequences (Figure 5), our data suggest specific target amino acid for the mutagenesis experiments. For example, dopamine D2 and D3 receptors that bind IgFLNa19 have significant homology with the FLN-binding site of GPIbα (Figure 5).[37] Since both GPIbα and integrins also associate with IgFLNa19 in vitro, it is highly possible that the D2 and D3 receptors share the same binding mode.

Structural basis of the different regulatory mechanism for FLNa-binding to the GPIb and integrin

The most striking specific feature of the GPIbα-IgFLNa17 complex is the interaction of Phe568 and Trp570 side chains with the main chain of the IgFLNa17 β strand C. These residues are not conserved in integrin tails. It has been recently shown that the mutations of these residues to alanines abrogate GPIbα binding to FLNa.[28] There might also be some specificity in the regulation of FLNa-integrin and FLNa-GPIbα interactions. While the integrin cytoskeleton interaction may be regulated by phosphorylation of Tyr or Thr residues of integrin tails,[38,39] such regulation cannot take place in the case of the GPIbα-FLNa interactions. The phosphorylated Tyr residue in the integrin tail is replaced by Phe in GPIbα, and the phosphorylated Thr residues are not conserved at all. On the other hand, our structure raises the possibility that phosphorylation of the GPIbα Ser565 might negatively regulate the interaction with FLNa because this Ser makes a side-chain hydrogen bond with the FLNa. A phosphate group in this position would be expected to prevent close contact between the peptide and FLNa. The GPIbα Ser566 is also a potential regulatory site, because dopamine D2 and D3 receptors have Ser residues at the same position (Figure 5) and the D2 S358D mutant receptor, which mimics its phosphorylation state, has lower affinity to FLNa

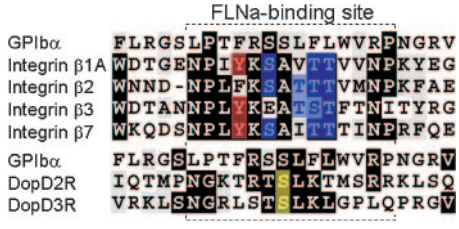

Figure 5. ClustalW alignment of GPIbα, integrin, and dopamine receptor cytoplasmic tail sequences. The FLNa-binding site of GPIbα and integrin β7 from the crystal structures and the corresponding sites of other integrins and dopamine D2 and D3 receptors are boxed. Potential phosphorylation sites (Tyr, red; Thr and Ser, blue) of integrins are indicated. A putative PKC phosphorylation site in D2 and D3 receptors are marked in yellow.

than wild type.[40] However, such phosphorylation of GPIbα has not been detected.

On the other hand, in vitro, the GPIbα-FLNa interaction can be dissociated by thiol alkylation with NEM.[32] Since there are no Cys residues in the cytoplasmic domain of the GPIbα, the GPIbα-interacting portion of FLNa should contain Cys modifiable by NEM. Crystal structure confirms this prediction: Cys1912 is in direct hydrophobic contact with GPIbα residue Leu567, while Cys1920 is located sufficiently close to the interface for its modifications to affect binding (Figure 2F). Both of these Cys residues are conserved in all 3 human isoforms of FLN (Figure 3A).

Topologic structure of the GPIb-FLNa complex and its biological significance

Isothermal titration calorimetry analysis showed that IgFLNa17 binds GPIbα556-577 peptide with a K_d in the micromolar range (Figure S1), demonstrating that the tightness of the complex[31] is not attributable to a single domain-domain interaction. Electron micrographs of the purified GPIb-FLNa complex and previous biochemical analyses support the general model of how FLNa interacts with the GPIb-IX-V complex (Figure 4A). To our knowledge, this is the first visualization of a native complex of a transmembrane receptor with a cytoskeletal protein. The micrographs support the general model derived indirectly of the overall structure of the complex, and suggest that the complex is stable as a monomeric unit in the resting platelet. Blood platelets maintain the GPIb-FLNa connection constitutively in both resting and activated states, including when subjected to high shear forces.[26] Clustering of this complex is induced by platelet activation and by chilling, which are important phenomena in thrombosis[41] and for transfusion medicine.[42] Therefore, we propose that the higher-order (or topologic) structure determines the tight-binding avidity of FLNa to the GPIb-IX-V receptor. This immediately means that clustering of the GPIb-IX-V complex and anchoring of FLNa to actin filaments by activation could also increase avidity, which could withstand high shear stress.

Acknowledgments

Dr Helena Tossavainen is acknowledged for her assistance with AMBER and CYANA calculations, and Dr Tiila Kiema for help in crystallography. We acknowledge the European Synchrotron Radiation Facility for provision of synchrotron radiation facilities, and thank Dr Didier Nurizzio for assistance in using the beamline ID23-1.

References

1. Flanagan LA, Chou J, Falet H, Neujahr R, Hartwig JH, Stossel TP. Filamin A, the Arp2/3 complex, and the morphology and function of cortical actin filaments in human melanoma cells. J Cell Biol. 2001;155:511-517.
2. Stossel TP, Condeelis J, Cooley L, et al. Filamins as integrators of cell mechanics and signalling. Nat Rev Mol Cell Biol. 2001;2:138-145.
3. van der Flier A, Sonnenberg A. Structural and functional aspects of filamins. Biochim Biophys Acta. 2001;1538:99-117.
4. Cunningham CC, Gorlin JB, Kwiatkowski DJ, et al. Actin-binding protein requirement for cortical stability and efficient locomotion. Science. 1992; 255:325-327.
5. Robertson SP. Molecular pathology of filamin A: diverse phenotypes, many functions. Clin Dysmorphol. 2004;13:123-131.
6. Feng Y, Walsh CA. The many faces of filamin: a versatile molecular scaffold for cell motility and signalling. Nat Cell Biol. 2004;6:1034-1038.
7. Andrews RK, Lopez JA, Berndt MC. Molecular mechanisms of platelet adhesion and activation. Int J Biochem Cell Biol. 1997;29:91-105.
8. Fox JE. Identification of actin-binding protein as the protein linking the membrane skeleton to glycoproteins on platelet plasma membranes. J Biol Chem. 1985;260:11970-11977.
9. Okita JR, Pidard D, Newman PJ, Montgomery RR, Kunicki TJ. On the association of glycoprotein Ib and actin-binding protein in human platelets. J Cell Biol. 1985;100:317-321.
10. Meyer SC, Zuerbig S, Cunningham CC, et al. Identification of the region in actin-binding protein that binds to the cytoplasmic domain of glycoprotein IBalpha. J Biol Chem. 1997;272:2914-2919.
11. Feng S, Resendiz JC, Lu X, Kroll MH. Filamin A binding to the cytoplasmic tail of glycoprotein Ibalpha regulates von Willebrand factor-induced platelet activation. Blood. 2003;102:2122-2129.
12. Williamson D, Pikovski I, Cranmer SL, et al. Interaction between platelet glycoprotein Ibalpha and filamin-1 is essential for glycoprotein Ib/IX receptor anchorage at high shear. J Biol Chem. 2002; 277:2151-2159.
13. Yap CL, Hughan SC, Cranmer SL, et al. Synergistic adhesive interactions and signaling mechanisms operating between platelet glycoprotein Ib/IX and integrin alpha IIbbeta 3: studies in human platelets and transfected Chinese hamster ovary cells. J Biol Chem. 2000;275:41377-41388.
14. Mannucci PM. Treatment of von Willebrand's disease. N Engl J Med. 2004;351:683-694.
15. Lopez JA, Andrews RK, Afshar-Kharghan V, Berndt MC. Bernard-Soulier syndrome. Blood. 1998;91:4397-4418.
16. Canobbio I, Balduini C, Torti M. Signalling through the platelet glycoprotein Ib-V-IX complex. Cell Signal. 2004;16:1329-1344.
17. Hoffmeister KM, Felbinger TW, Falet H, et al. The clearance mechanism of chilled blood platelets. Cell. 2003;112:87-97.
18. Feng S, Lu X, Kroll MH. Filamin A binding stabilizes nascent glycoprotein Iba trafficking and thereby enhances its surface expression. J Biol Chem. 2005;280:6709-6715.
19. Guntert P. Automated NMR protein structure calculation. Prog Nucl Magn Reson Spectroscopy. 2003;43:105-125.
20. Herrmann T, Guntert P, Wuthrich K. Protein NMR structure determination with automated NOE assignment using the new software CANDID and the torsion angle dynamics algorithm DYANA. J Mol Biol. 2002;319:209-227.
21. Kabsch W. Automatic processing of rotation diffraction data from crystals of initially unknown symmetry and cell constants. J Appl Crystallogr. 1993;26:795-800.
22. Storoni LC, McCoy AJ, Read RJ. Likelihood-enhanced fast rotation functions. Acta Crystallogr D Biol Crystallogr. 2004;60:432-438.
23. Perrakis A, Morris R, Lamzin VS. Automated protein model building combined with iterative structure refinement. Nat Struct Biol. 1999;6:458-463.
24. Jones TA, Zou J-Y, Cowan SW, Kjeldgaard M. Improved methods for the building of protein models in electron density maps and the location of errors in these models. Acta Crystallogr A. 1991;47:110-119.
25. Murshudov GN, Vagin AA, Dodson EJ. Refinement of macromolecular structures by the maximum-likelihood method. Acta Crystallogr D Biol Crystallogr. 1997;53:240-255.
26. Kovacsovics TJ, Hartwig JH. Thrombin-induced GPIb-IX centralization on the platelet surface requires actin assembly and myosin II activation. Blood. 1996;87:618-629.
27. Gorlin JB, Yamin R, Egan S, et al. Human endothelial actin-binding protein (ABP-280, nonmuscle filamin): a molecular leaf spring. J Cell Biol. 1990; 111:1089-1105.
28. Cranmer SL, Pikovski I, Mangin P, et al. Identification of a unique filamin A binding region within the cytoplasmic domain of glycoprotein Ibalpha. Biochem J. 2005;387:849-858.
29. Pudas R, Kiema TR, Butler PJ, Stewart M, Ylänne J. Structural basis for vertebrate filamin dimerization. Structure (Camb). 2005;13:111-119.
30. Ezzell RM, Kenney DM, Egan S, Stossel TP, Hartwig JH. Localization of the domain of actin-binding protein that binds to membrane glycoprotein Ib and actin in human platelets. J Biol Chem. 1988;263:13303-13309.
31. Thompson JD, Higgins DG, Gibson TJ. CLUSTAL W: improving the sensitivity of progressive multiple sequence alignment through sequence weighting, position-specific gap penalties and weight matrix choice. Nucleic Acids Res. 1994; 22:4673-4680.
32. Berndt MC, Gregory C, Kabral A, Zola H, Fournier D, Castaldi PA. Purification and preliminary characterization of the glycoprotein Ib complex in the human platelet membrane. Eur J Biochem. 1985; 151:637-649.
33. Fox JE, Aggerbeck LP, Berndt MC. Structure of the glycoprotein Ib.IX complex from platelet membranes. J Biol Chem. 1988;263:4882-4890.
34. Solum NO, Clemetson KJ. The discovery and characterization of platelet GPIb. J Thromb Haemost. 2004;3:1125-1132.
35. Xu W, Xie Z, Chung DW, Davie EW. A novel human actin-binding protein homologue that binds to platelet glycoprotein Ibalpha. Blood. 1998;92: 1268-1276.
36. Takafuta T, Wu G, Murphy GF, Shapiro SS. Human beta-filamin is a new protein that interacts with the cytoplasmic tail of glycoprotein Ibalpha. J Biol Chem. 1998;273:17531-17538.

37. Li M, Bermak JC, Wang ZW, Zhou QY. Modulation of dopamine D(2) receptor signaling by actin-binding protein (ABP-280). Mol Pharmacol. 2000; 57:446-452.

38. Tapley P, Horwitz A, Buck C, Duggan K, Rohrschneider L. Integrins isolated from Rous sarcoma virus-infected chicken embryo fibroblasts. Oncogene. 1989;4:325-333.

39. Valmu L, Fagerholm S, Suila H, Gahmberg CG. The cytoskeletal association of CD11/CD18 leukocyte integrins in phorbol ester-activated cells correlates with CD18 phosphorylation. Eur J Immunol. 1999;29:2107-2118.

40. Li M, Li C, Weingarten P, Bunzow JR, Grandy DK, Zhou QY. Association of dopamine D(3) receptors with actin-binding protein 280 (ABP-280). Biochem Pharmacol. 2002;63:859-863.

41. Celikel R, McClintock RA, Roberts JR, et al. Modulation of alpha-thrombin function by distinct interactions with platelet glycoprotein Ibalpha. Science. 2003;301:218-221.

42. Hoffmeister KM, Josefsson EC, Isaac NA, Clausen H, Hartwig JH, Stossel TP. Glycosylation restores survival of chilled blood platelets. Science. 2003;301:1531-1534.

43. Berman HM, Westbrook J, Feng Z, et al. The Protein Data Bank. Nucleic Acids Res. 2000;28:235-242. http://www.pdb.org. Accessed January 4, 2006.

44. Seavey BR., Farr EA, Westler WM, Markley JL. A relational database for sequence-specific protein NMR data. J Biomol NMR. 1991;1:217-236. http://www.bmrb.wisc.edu. Accessed January 4, 2006.

45. Kiema T, Lad Y, Jiang P, et al. The molecular basis of filamin binding to integrins and competition with talin. Mol Cell. In press.